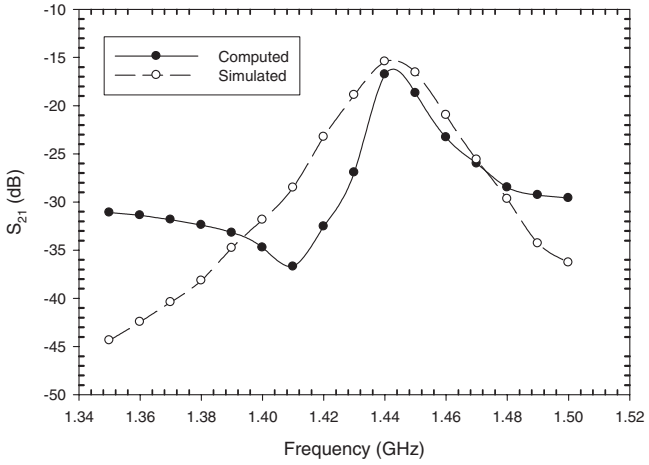

Figure 6 Variation of mutual coupling with frequency for circular patches with center short. $\varepsilon_r = 2.5$, $r_1 = r_2 = 38.5$ mm, $h = 1.575$ mm, $s = 4$ mm

tween gap-coupled circular microstrip patches. A class of circular patches is analyzed, which includes unloaded patch and patches with sort. The comparison of measured and simulated results shows reasonable accuracy. The closed-form expressions are easy to compute and will offer the design engineer an accurate estimation of mutual coupling.

REFERENCES

1. G. Kumar and K.C. Gupta, Broadband microstrip antennas using additional resonators gap coupled to the radiating edges, IEEE Trans Antennas Propag 32 (1984), 1375-1379.
2. E.H. Van Lil and A.R. Vande Capelle, Transmission line model for mutual coupling between microstrip antennas, IEEE Trans Antennas Propag 32 (1984), 816-821.
3. K. Mahdjoubi, E. Penard, J.P. Daniel, and C. Terret, Mutual coupling between circular disc microstrip antennas, Electron Lett 23 (1987), 27-28.
4. J.T. Aberie and D.M. Pozar, A full-wave solution for the mutual coupling between circular microstrip antennas, Microwave Opt Technol Lett 2 (1989), 130-132.
5. C.-Y. Huang and K.-L. Wong, Mutual coupling computation of probe-fed circular microstrip antennas, Microwave Opt Technol Lett 19, 100-102, 1998.
6. L. Vegni, A. Toscano, and F. Bilohi, Mutual coupling between circular patch antennas integrated in an inhomogeneous grounded slot, Microwave Opt Technol Lett 25, 294-297, 2000.
7. R.P. Jedlicka, M.T. Poe, and K.R Carver, Measured mutual coupling between microstrip antennas, IEEE Trans Antennas Propag 29 (1981), 147-149.
8. N. Kumprasart and W. Kiranon, Simple and accurate formula for the resonant frequency of the circular microstrip disk antenna, IEEE Trans Antennas Propag 43 (1995), 1331-1333.
9. R. Garg, P. Bhartia, I. Bahl, and A. Ittipiboon, Microstrip antenna design handbook, Artech House Publishers, Boston, London, 2001.

© 2008 Wiley Periodicals, Inc.

PRINTED SYMMETRIC INVERTED-F ANTENNA WITH A QUASI-ISOTROPIC RADIATION PATTERN

Chihyun Cho,[1] Hosung Choo,[1] and Ikmo Park[2]
[1] School of Electronic and Electrical Engineering, Hongik University, 72-1 Sangsu-Dong, Mapo-Gu, Seoul 121-791, Korea; Corresponding author: hschoo@hongik.ac.kr
[2] Department of Electrical and Computer Engineering, Ajou University, 5 Wonchon-Dong, Youngtong-Gu, Suwon 443-749, Korea

Received 6 September 2007

ABSTRACT: *This article presents a tag antenna with a quasi-isotropic radiation pattern operating in the UHF band to eliminate the shadow zone in RFID systems. The proposed tag antenna has a symmetric inverted-F structure with a bent section and is printed on a 50 μm-thick PET substrate for easy and low-cost fabrication. The detailed design parameters of the antenna were optimized using a Pareto genetic algorithm in conjunction with the IE3D EM simulator. The optimized antenna shows 3.2% fractional bandwidth for $S_{11} < -10$ dB, more than 87% efficiency in the operating frequency band, and less than 6 dB gain deviation. The measured reading range between the tag and reader is between 1.4 and 2.2 m.* © 2008 Wiley Periodicals, Inc. Microwave Opt Technol Lett 50: 927–930, 2008; Published online in Wiley InterScience (www.interscience.wiley.com). DOI 10.1002/mop.23247

Key words: *RFID; tag antenna; isotropic radiation pattern; inverted-F*

1. INTRODUCTION

Generally, an antenna for the reader in RFID systems uses circular polarization to ensure tag detection independent of the incoming wave's polarization [1, 2]. While the most common antenna structure for tags is a linearly polarized antenna, such as a dipole or a loop [3-7]. However, such antennas usually have nulls or very low gains in certain directions in their radiation patterns. If the tag points to the reader through one of those nulls, then the reading range of the tag decreases drastically or, in the worst case, the reader might not even detect the tag at all. This is one of the primary factors hindering the stability of the RFID system, and in some applications the stable readability is extremely critical [8]. To alleviate this problem, a tag antenna should have a nearly isotropic radiation pattern, and at the same time maintain a planar structure for easy and low-cost fabrication.

In this article, a planar tag antenna with a quasi-isotropic radiation pattern is designed using a symmetric inverted-F structure with a bent section. The designed tag antenna uses two orthogonally directed electric currents to achieve a quasi-isotropic radiation pattern by compensating the nulls of each other. The impedance of the tag antenna is conjugate-matched to the commercial tag chips, which usually have very large reactive values [7, 9, 10]. The proposed antenna was found to have a fractional bandwidth of 3.2% ($S_{11} < -10$ dB), an efficiency of 87%, and a gain deviation of less than 6 dB over all the directions based on measurement. The measured maximum reading range between the tag and the reader falls in between 1.4 and 2.2 m, depending on the rotation angle of the tag. These results verify the elimination of the shadow zone in the reading pattern of the designed tag antenna.

2. ANTENNA STRUCTURE AND CHARACTERISTICS

The proposed antenna structure is shown in Figure 1. The antenna consists of a symmetric planar inverted-F and bent sections. The conducting part of the antenna is printed on thin polyethylene (PET: $\varepsilon_r = 3.9$ and $\tan\delta = 0.003$ in the UHF band) substrate for easy and low-cost fabrication. The input impedance of the passive

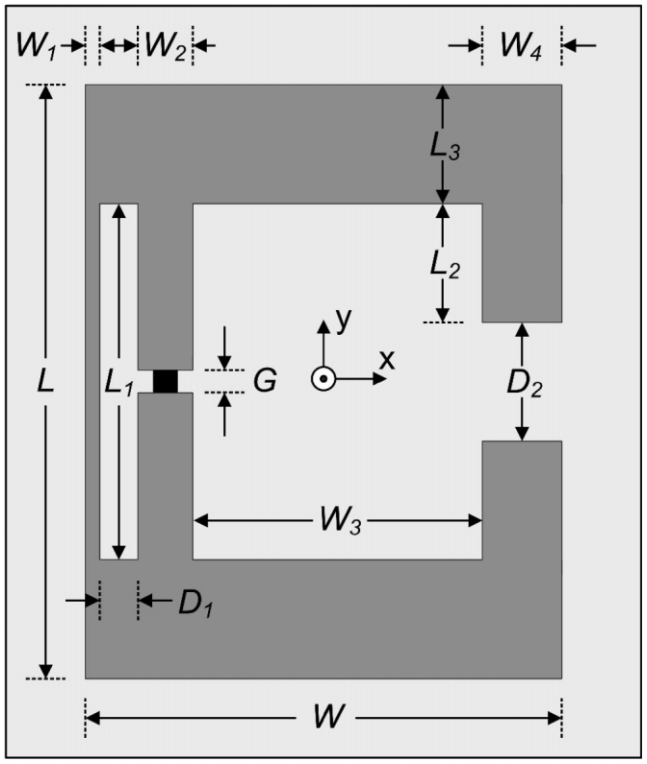

Figure 1 Structure of the proposed antenna and the design parameters

tag chip is usually very capacitive since the tag chips typically include a rectifier to accumulate DC power for operation of inner circuits [7-10]. Therefore, the input impedance of the tag antenna should be designed to have an appropriate inductive value for conjugate matching [4-8]. The proposed planar symmetric inverted-F structure has a strong advantage in regard to reactive matching, since the matching stub on the left side of the feed in Figure 1 can be utilized to control the inductance of the antenna by changing the size of the feed loop formed by L_1 and D_1. In addition, the end sections of the antenna formed by W_4 and L_2 are bent thereby efficiently allowing a reduction in the antenna size and tuning of the reactive value by capacitive loading. The orthogonally directed currents that flow in the x-direction (through section W) and y-direction (through sections L, L_1, and L_2), respectively, produce radiation patterns each of which can compensate the radiation nulls of the other, thus making it possible to achieve a quasi-isotropic radiation pattern [11, 12].

To determine the detailed design parameters that yield the best conjugate matching with a quasi-isotropic radiation pattern for the planar symmetric inverted-F structure, the Pareto genetic algorithm (GA) [13-15] was used in conjunction with an IE3D full-wave EM simulator [16]. The three design goals used in the Pareto GA optimization were as follows: (1) high EB (efficiency-bandwidth product), (2) small antenna size, and (3) small gain deviation in their radiation patterns. Specifically, the gain deviation was required to be less than 1/4 (6 dB) of its maximum gain along arbitrary directions to achieve deviation of the reading range of less than 1/2 of its maximum value [8]. After 400 iterations of the GA process, the design parameters converged on the following dimensions: $W = 60.2$ mm, $L = 76.6$ mm, $L_1 = 46.6$ mm, $L_2 = 15.7$ mm, $L_3 = 15.0$ mm, $D_1 = 2.1$ mm, $D_2 = 15.2$ mm, $W_1 = 1.5$ mm, $W_2 = 5.0$ mm, $W_3 = 42.0$ mm, and $W_4 = 9.6$ mm. Figure 2 shows the resulting return loss, both simulated and measured, of the optimized antenna when it is connected to a commercial tag

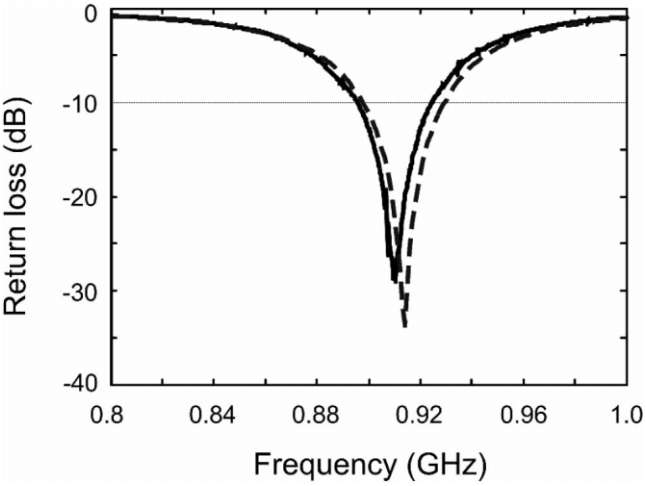

Figure 2 Return loss as a function of frequency for the optimized antenna. The dashed line (- - -) represents the simulated result and the solid line (—) represents the measured result

chip (ALL 9238, 9250 [17]) with an input impedance of about 13-j135 at 914 MHz. The measured and simulated bandwidths ($S_{11} < -10$ dB) are about 3.2% (895~924 MHz) and 3.4% (898~929 MHz), respectively, and their agreements are apparent. To explain the impedance matching characteristics of the proposed antenna, the input impedance was modeled using a lumped RLC circuit, as shown in Figure 3(a). The matching stub on the left side of the planar symmetric inverted-F antenna was represented as an induc-

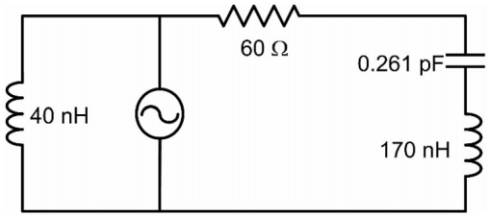

(a)

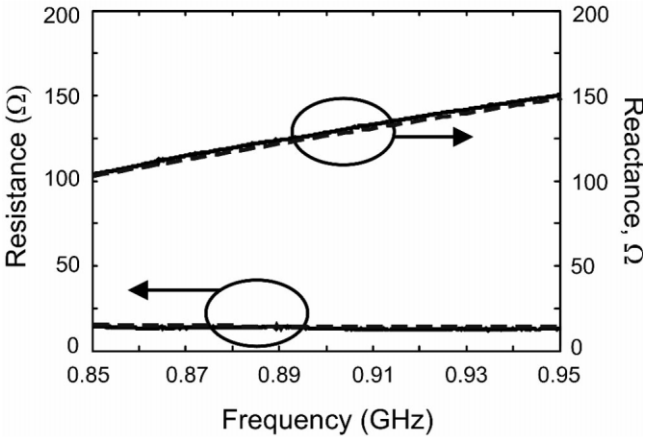

(b)

Figure 3 A circuit model of the optimized antenna. The solid line (—) represents the measured impedance data and the dashed line (- - -) is the calculated impedance data based on the circuit model

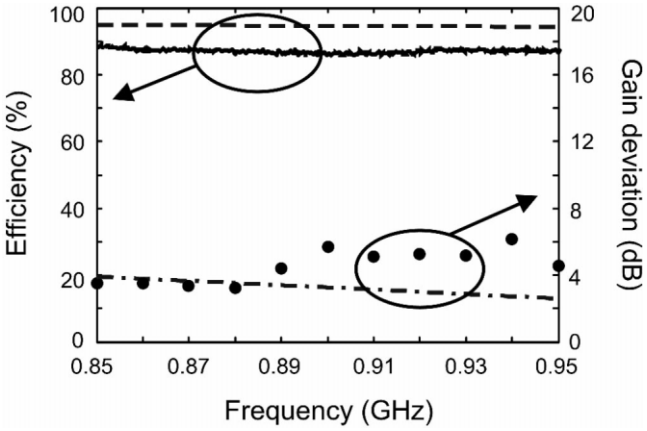

Figure 4 Efficiency and gain deviation as a function of frequency for the optimized antenna. The dashed line (- - -) is the simulated efficiency and the solid line (—) is the measured efficiency. The dash-dotted line (●) is the simulated gain deviation and the circles (λ) are the measured gain deviation

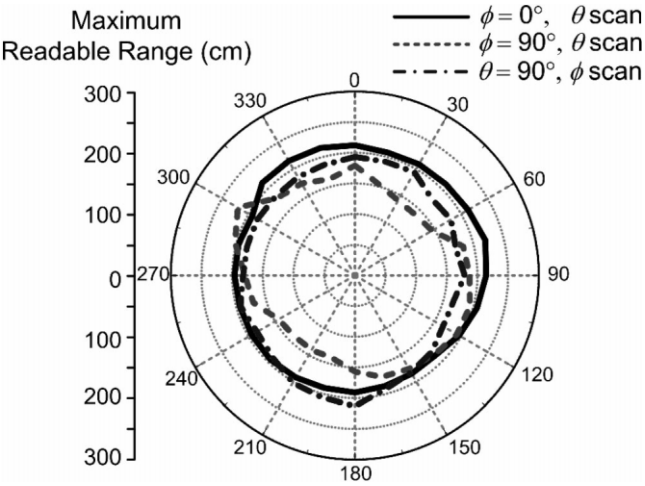

Figure 6 Reading pattern of the optimized antenna

tor and the remaining parts of the antenna were modeled with a series RLC circuit. The value of each lumped element was obtained first by simulating each part of the antenna separately using the IE3D simulator and then by further tuning it to fit the measured value. The impedance obtained using both the circuit model and the measurement is shown in Figure 3(b). Again, this result shows that the matching stub can be used to easily control the input reactance of the antenna by changing the size of the feed loop, while still maintaining the input resistance. For instance, as the feed loop is increased by expanding D_1, the reactance of the antenna is raised with only a small change in its resistance. Hence, the planar symmetric inverted-F antenna structure offers great flexibility in conjugate matching when dealing with various commercial tag chips having large capacitive values.

Figure 4 shows the radiation efficiency and gain deviation as a function of frequency. The simulated and measured efficiencies are represented by the dashed and solid lines, respectively. The measurement was achieved using the Wheeler cap method as described in [18-20], and the result shows values in excess of 87% in the frequency range of operation. The dash-dotted line and circles represent the simulated and measured gain deviation, respectively. Both the simulation and measurement results show a nearly isotropic pattern with the gain deviation of less than 6 dB between 850 and 950 MHz. Figure 5 shows the measured gain at the frequency of 914 MHz which also shows a radiation pattern that is close to being isotropic. We also measured the maximum reading range between the proposed tag antenna mounted on a commercial tag chip and the reader [17], the result of which is represented in Figure 6. The solid, dashed, and dash-dot lines represent the measured values on the xz-, yz-, and xy-plane, respectively. The measured maximum reading range in any arbitrary direction was between 1.4 and 2.2 m.

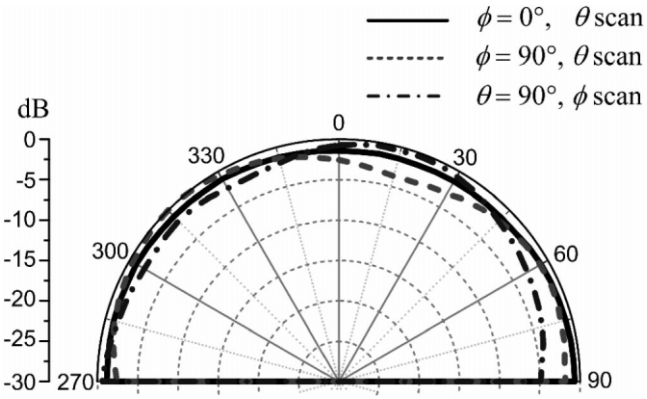

Figure 5 Normalized total gain of the optimized antenna

To explain the radiation characteristics of the proposed antenna, we examined the radiation pattern due to the individual current distribution on each part of the antenna body. Figures 7(a) and 7(b) display the respective radiation patterns due to the *x*-directed (throw section *W*) and *y*-directed (throw sections *L*, L_1, and L_2) currents only. The *y*-directed currents produce the doughnut shaped radiation pattern of a dipole that has a radiation null in the *y*-direction. By contrast, the *x*-directed currents produce a strong radiation in the *y*-direction since the currents on upper and lower sides of the antenna flow in opposite directions with an equal amplitude, and therefore the radiation pattern on the xz-plane is canceled out while producing a strong radiation field in the *y*-axis direction. Therefore, the two radiation patterns of the orthogonally directed currents each compensate the nulls of the other, enabling a quasi-isotropic radiation pattern.

3. CONCLUSION

In this article, we designed a tag antenna with a quasi-isotropic radiation pattern using a planar symmetric inverted-F structure. The proposed antenna can produce a good conjugate impedance matching with a commercial tag chip by adjusting the size of the matching stub and the bent section of the antenna. In addition, the antenna shows a quasi-isotropic radiation pattern using orthogonal surface currents distributions. Hence, the proposed antenna eliminates the shadow zone and improves the stability of RFID systems. The detailed design parameters of the antenna were optimized using a Pareto GA in conjunction with an IE3D EM simulator. The optimized antenna has a fractional bandwidth of 3.2% and an efficiency of 87% at the operating frequency. The measured gain deviation is less than 6 dB from 850 to 950 MHz. We also used a lumped RLC circuit model and radiation patterns produced by individual orthogonal surface currents to explain the operating principle of the proposed tag antenna. The measured maximum reading range of a tag with a commercial chip and reader was between 1.4 and 2.2 m for any arbitrary direction.

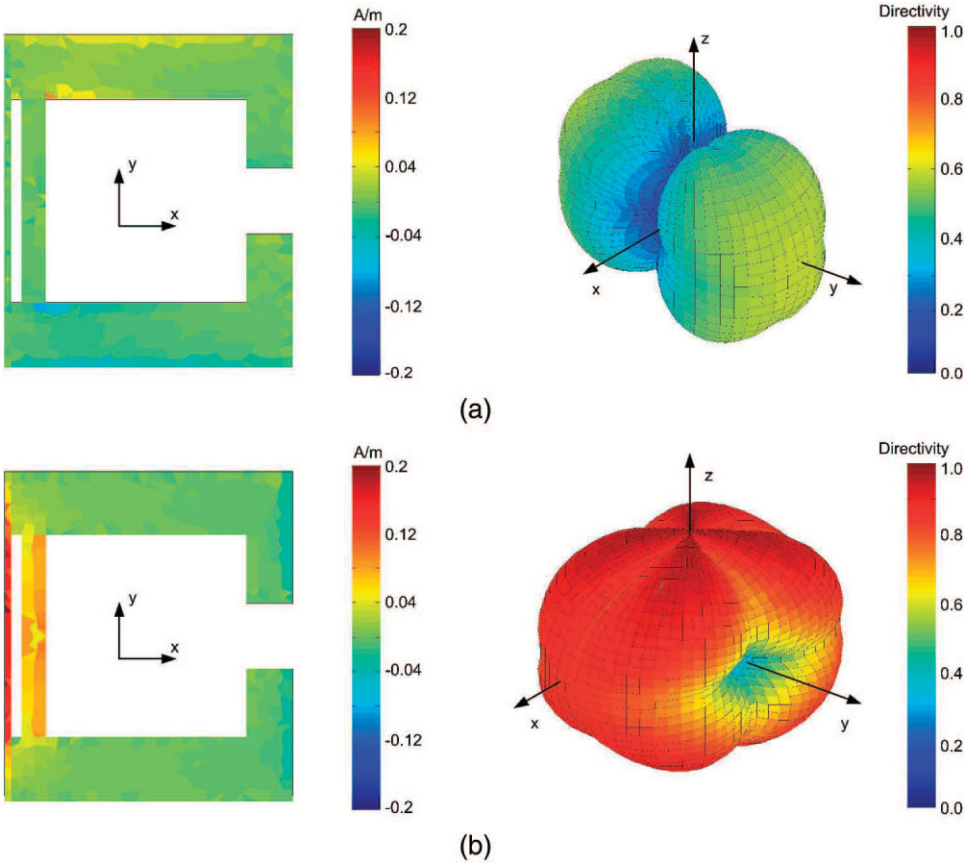

Figure 7 Normalized radiation pattern. (a) Radiation pattern due to x-directed currents, (b) radiation pattern due to y-directed currents. [Color figure can be viewed in the online issue, which is available at www.interscience.wiley.com]

ACKNOWLEDGMENTS

This research was supported by the Seoul R&BD program in Korea.

REFERENCES

1. K. Finkenzeller, RFID handbook, 2nd ed., Wiley, West Sussex, England, 2003.
2. P.Y. Lau, H. Wong, and E.K.N. Yung, Accordion shape monofilar axial mode helix for RFID reader, Electron Lett 42 (2006), 607-608.
3. M. Keskilammi and M. Kivikoski, Using text as a meander line for RFID transponder antennas, IEEE Antennas Wireless Propag Lett 3 (2004), 372-374.
4. M. Ritamaki, A. Ruhanen, V. Kukko, J. Miettinen, and L.H. Turner, Contactless radiation pattern measurement method for UHF RFID transponders, Electron Lett 41 (2005), 723-724.
5. Y. Tikhov and J.H. Won, Impedance-matching arrangement for microwave transponder operating over plurality of bent installation of antenna, Electron Lett 40 (2004), 574-575.
6. P.V. Nikitin, K.V.S. Rao, S.F. Lam, V. Pillai, R. Martinez, and H. Heinrich, Power reflection coefficient analysis for complex impedances in RFID tag design, IEEE Trans Microwave Theory Tech 53 (2005), 2721-2725.
7. K.V.S. Rao, P.V. Nikitin, and S.F. Lam, Antenna design for UHF RFID tags: a review and a practical application, IEEE Trans Antenn Propag 53 (2005), 3870-3876.
8. C. Cho, H. Choo, and I. Park, Broadband RFID tag antenna with quasi-isotropic radiation pattern, Electron Lett 41 (2005), 1091-1092.
9. U. Karthaus and M. Fischer, Fully integrated passive UHF RFID transponder IC with 16.7-μW minimum RF input power, IEEE J Solid-State Circ 38 (2003), 1602-1608.
10. J.-P. Curty, N. Joehl, C. Dehollain, and M.J. Declercq, Remotely powered addressable UHF RFID integrated system, IEEE J Solid-State Circ 40 (2005), 2193-2202.
11. K. Fujimoto, A. Henderson, A. Hirasawa, and J.R. James, Small antennas, Research Studies Press, distributed by Wiley, New York, 1987.
12. C. Soras, M. Karaboikis, G. Tsachtsiris, and V. Makios, Analysis and design of an inverted-F antenna printed on a PCMCIA Card for the 2.4 GHz ISM band, IEEE Antenn Propagat Mag 44 (2002), 37-44.
13. D.E. Goldberg, Genetic algorithms in search, optimization and machine learning, Addison-Wesley, Reading, MA, 1989.
14. Y. Rahmat-Samii and E. Michielssen, Electromagnetic optimization by genetic algorithms, Willey, New York, 1999.
15. T. Hiroyasu, M. Miki, and S. Watanabe, The new model of parallel genetic algorithm in multi-objective optimization problems—Divided range multi-objective genetic algorithm, Proc Congress Evol Comput 1 (2000), 333-340.
16. Zeland Software Inc., IE3D simulator, Fremont, CA Jan 2007.
17. RFID system. Available at http://www.alientechnology.com.
18. H.A. Wheeler, The radiansphere around a small antenna, Proc IRE 47 (1959), 1325-1331.
19. G.S. Smith, An analysis of the Wheeler method for measuring the radiation efficiency of antennas, IEEE Trans Antenn Propag 25 (1997), 552-556.
20. H. Choo, R. Rogers, and H. Ling, On the Wheeler cap measurement of the efficiency of microstrip antennas, IEEE Trans Antenn Propag 53 (2005), 2328-2332.

© 2008 Wiley Periodicals, Inc.